Keywords
electrochemical impedance, nanoporous gold, breakpoint frequency

Characterization of the Effect of Film Thickness on the Electrochemical Impedance of Nanoporous Gold

Nicholas C. Bell, James G. Collins, and Ryan M. Turner

Virginia Polytechnic Institute and State University
Department of Materials Science and Engineering
213 Holden Hall, Virginia Tech
Blacksburg, Virginia 24061

Abstract

Graphs are generated characterizing the effect of film thickness on the electrochemical impedance of nanoporous gold. Twelve-karat white gold (50% Ag, 50% Au) leaves were dealloyed to make a total of 12 nanoporous gold samples from 100-300 nm thick. Scanning electron microscopy (SEM) was used to determine the pore diameter distributions and an electrochemical cell was used to collect impedance data for each sample. Analysis of the SEM micrographs shows the pore morphology ranges from shallow spherical pores to deep interconnected pores, and the diameter distributions were between 10 nm and 20 nm for all of the samples. A linearized graph of impedance |Z| versus frequency shows that the breakpoint frequency decreases with increasing film thickness. Below the breakpoint frequency, the data support an idealized model that assumes through-thickness pores with uniform diameters. Above the breakpoint frequency, however, the ideal model predicts a drastic impedance decrease, whereas the data show only a slight impedance decrease.

1. Introduction

Industry currently uses nanoporous metals in several applications, such as leads in cardiac pacemakers, because they provide large surface area at reduced material mass. For example, cardiac pacing leads are coated with a nanoporous metal layer that conducts electrical signals to the heart through saline-like body fluids.[1,2,3] These metals have relatively high electrical impedances that lower the stimulating current to the heart. Little is understood, however, about the effect of film thickness on the leads' electrical properties, such as impedance. Current literature about nanoporous metals discusses only the composition and dissolution potential necessary for creating pores.[4,5,6] Characterizing the effect of film thickness on a nanoporous metal's electrochemical impedance could help manufacturers control performance characteristics such as longevity more closely.

1.1 Nanoporous Gold

Although platinum is a typical component of pacing leads, gold provides a nanoporous model analogous to a platinum system. Gold is a model alloy system composed of a single phase alloy over the entire composition range, with

only 0.2% lattice misfit between Ag and Au. This low misfit allows structural changes to be ignored when Ag is selectively dissolved from Au in dealloying.[3] Additionally, gold is less expensive than platinum and is readily accessible and much easier to process, making it ideal for preliminary modeling.

Nanoporous metals used for cardiac pacing leads are produced through dealloying, in which the most electrochemically active element of an alloy is parted through selective dissolution.[1,2,4-7] This selective dissolution produces a sponge-like nanoporous structure of the more noble alloy element.[5] Early in the process of dealloying silver from an Ag-Au alloy, the gold clusters form mounds with gold-rich peaks on the surface and bases that resemble the starting alloy. Further dissolution attacks the bases of the mounds and creates pits that contribute to the nanoporosity of the alloy.[1,5,6]

1.2 Impedance Theory

Impedance is a material's ability to slow down the flow of electrical current. For pacemaker applications, higher lead impedance lowers the current needed to stimulate the heartbeat, which extends the battery life. Equation 1 shows the relationship between

$$I_l = \frac{V_0^2 t}{V_b Z_p L} \qquad (1)$$

pacing impedance and current seen by the patient: where I_l is the current delivered to the patient, Z_p is the pacing impedance, V_o is the output voltage, V_b is the battery voltage, t is time, and L is cycle length.[1] The battery produces an alternating current (AC) of varying frequencies, and the frequency depends on pore size, shape, and distribution for nanoporous metals.[1] Therefore, impedance depends on porosity.

The breakpoint frequency is the frequency at which the current passes through the pore surface area of the nanoporous metal, and the metal no longer acts like a continuous, polished material. Because apparent surface area in the nanoporous metal increases substantially, impedance rises sharply as frequency decreases. However, above the breakpoint frequency, the current passes over the lead as though it had a polished surface and consequently lowers the overall impedance of the lead.[1] In addition, increasing porous layer thickness will decrease the lead's impedance and shift the breakpoint frequency to a smaller value.[1] Lowering the breakpoint frequency allows a lower AC current frequency to be used to achieve a given impedance compared to nanoporous materials with higher breakpoint frequencies or polished, continuous materials.

To facilitate control of impedance characteristics, this research analyzes the effect of film thickness on the electrochemical impedance of nanoporous gold. Changes in breakpoint frequencies for various film thicknesses were analyzed to determine a procedure for lowering the breakpoint frequencies of nanoporous gold and to model this effect to predict impedance behavior for other film thicknesses.

2. Experimental Procedure

2.1 Nanoporous Gold Sample Preparation

Each nanoporous gold sample was made by dealloying 12-karat, 100 nm thick Monarch white gold leaf (50 wt. % Au, 50 wt. % Ag) manufactured by Sepp Leaf Products, Inc. First, the leaf was rolled onto a graphite rod and unrolled into a dish of de-ionized (DI) water to make the leaf taut. After rolling the leaf back onto the graphite rod, it was unrolled into a dish filled with 0.1 M HNO_3 and allowed to dealloy for five minutes.

Next, the nanoporous foil was rolled onto the graphite rod and unrolled into a dish of DI water. Foil transfer from one DI water bath to another continued four more times for thorough foil washing. Then, a piece of clean silicon wafer was submerged beneath the foil and lifted out of the DI water with some of the foil adhered to it, after which the foil was dried to the wafer in a general purpose Precision™ oven at 145°C for 10 minutes. Sample thicknesses were produced with thicknesses of 100 nm, 200 nm, and 300 nm. Film thickness was increased by adding another gold foil to a foil already adhered to a silicon wafer. The use of silicon wafers with oxide layers was avoided because oxide layers prevent film thickness stacking. Since heating silicon wafers creates oxide, unnecessary sample heating was avoided as well. Overall, a total of 12 samples were created with four samples for each film thickness.

Scanning electron microscopy (SEM) specimens were prepared by using a diamond-tipped scriber to remove a small section from each sample. The SEM specimens were viewed using a LEO® 1550 SEM at

a magnification of 300k with an accelerating voltage of 5 kV. All samples were stored in a humidity-controlled nitrogen cabinet.

2.2 Electrochemical Impedance Testing

Electrochemical impedance tests were performed on samples not viewed with SEM using a three-electrode electrochemical cell set-up at room temperature. A KIMAX® crystallizing dish with a 170 mL maximum capacity was filled about ¾-full with 0.1 M $HClO_4$. The dish was placed on a platform lift on the base of a stand. Alligator clips attached to a Gamry® Potentiostat were suspended from the stand's clamps. A saturated mercury/mercurous sulphate (MSE) reference electrode was suspended from one clamp, whereas a platinum foil counter electrode was attached with an alligator clip to another clamp. A copper lead was attached to the sample to be tested using Teflon tape with the lead making sufficient contact with the nanoporous gold foil to create the third electrode.

Using the platform lift, the dish containing the $HClO_4$ was raised to submerge all three electrodes in the acid. Before submerging the sample, the surface area of the part of the sample to be tested was approximated with a caliper, and the edges of that area were covered with a small amount of DI water to ensure that the $HClO_4$ did not peel the foil from the wafer as it submerged. Each test was run using Gamry Instruments® Framework 3.20 electrochemical testing software. First, the DC voltage potential was held at the open circuit potential while an AC potential of 10 mV rms was applied across that part of the sample submerged in the $HClO_4$. After entering the approximated surface area, the impedance test ran from frequencies of 0.2 to 1E6 Hz. The results were viewed using ZView 2.3d (by Scribner Associates, Inc.) from which the data were extracted and imported into spreadsheet software for analysis.

2.3 Data Analysis

Pore diameter distributions were determined by using image threshold software on the SEM micrographs. The software creates a dark/light contrast between the pores and the ligaments, measuring the diameter of the dark areas (the pores). The results were used to create histograms showing the pore diameter distributions.

Graphing software was used to generate graphs of the impedance magnitude |Z| (ohms) versus frequency (Hz) in log-log coordinates for each film thickness to estimate where each curve's slope changes (i.e., the breakpoint frequency). The impedance data were imported into spreadsheet software, which was used to calculate the average |Z| for each film thickness. The point-slope method was used to create a linear curve with a distinct slope change for each film thickness. A more specific breakpoint frequency exists where the slope changes for each curve. The spreadsheet software was also used to calculate the standard deviation between the breakpoint frequencies of the samples for each film thickness.

3. Results and Discussion

3.1 SEM Micrographs of Pore Morphology

SEM micrographs of each sample were obtained to confirm pore morphology and distribution of pore sizes in the nanoporous gold. Pore morphology ranges from roughly spherical pores to interconnected pores, as seen on the surface of the 100 nm thick sample shown in Figure 1. Figure 2 is the pore size distribution for a 100 nm thick gold sample and indicates the pore sizes are in the expected range for a dealloying time of 5 minutes in HNO_3.

The majority of the pore diameters fall between 10 nm and 20 nm. SEM micrographs and pore size distributions of the 4 samples for each thickness (100 nm, 200 nm, 300 nm) indicate a consistent pore diameter and pore morphology among all 12 samples.

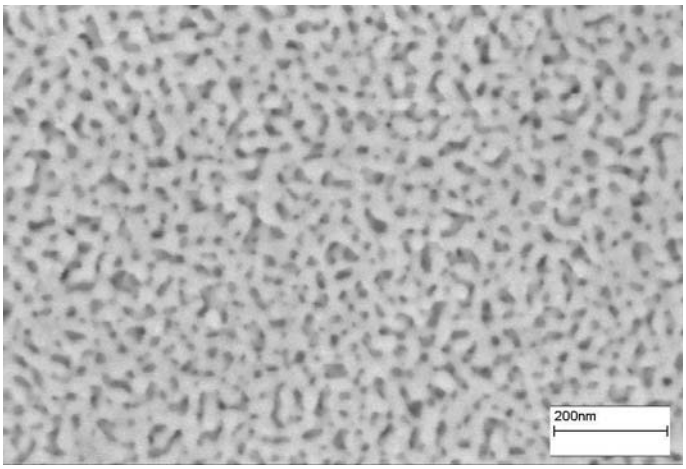

Figure 1. SEM micrograph of a 100nm thick nanoporous gold sample on a Si [110] substrate

3.2 Film Thickness Effects on Breakpoint Frequency

Figure 3 plots the average |Z| versus frequency of the four samples tested for each film thickness, showing a distinct slope change between the background (the region of the curve at the lower frequencies) and the foreground (the region of the curve at the higher

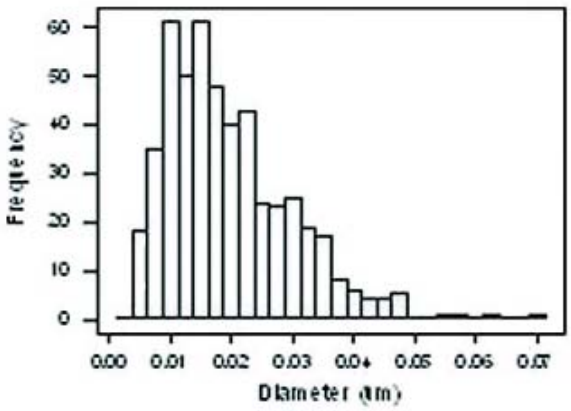

Figure 2. Pore size distribution of a 100 nm thick nanoporous gold sample on a Si [110] substrate

frequencies). Figure 4 displays a linearized version of Figure 3 in which the linearity of the background and foreground for each curve is enhanced to find a specific breakpoint frequency, denoted by the circles. Overall, Figure 3 shows that an inverse relationship exists between film thickness and breakpoint frequency for nanoporous metals: as film thickness increases, breakpoint frequency decreases.

The average breakpoint frequencies are 34.0, 28.5, and 11.98 Hz for the 100 nm, 200 nm, and 300 nm film thickness, respectively. The standard deviation

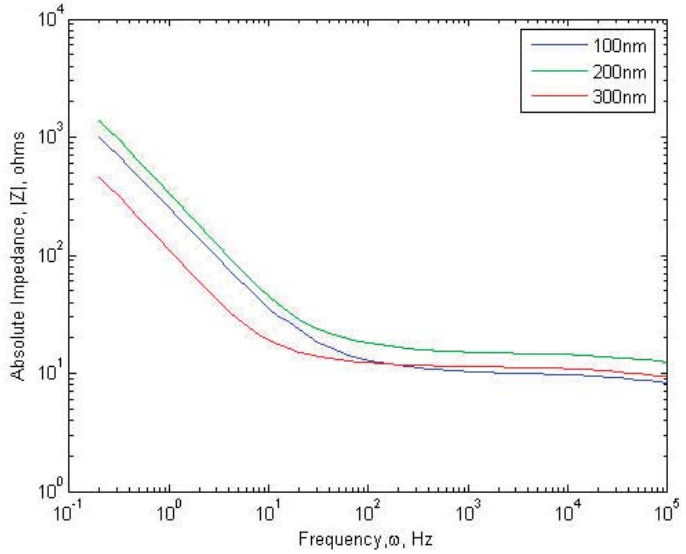

Figure 3. Real impedance vs. frequency data

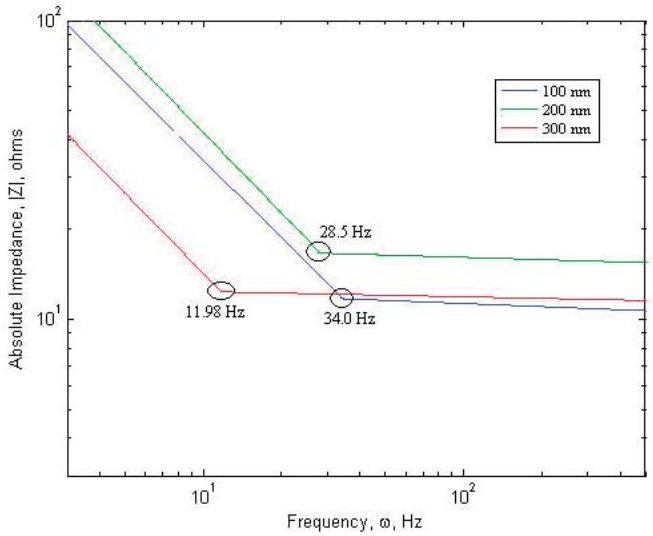

Figure 4. Calculated breakpoint frequencies for real impedance data

is 7.4, 2.1, and 1.3 Hz for the 100 nm, 200 nm, and 300 nm film thickness, respectively. Consequently, the 100 nm data range overlaps that of the 200 nm film thickness. Additional testing should decrease the standard deviation of the 100 nm film thickness data and refine the model.

3.3 Comparison to Existing Models

The ideal model from Dr. Pugh's thesis[1] (and shown in Figure 5) was based upon the De Levie equation typically cited in literature. It suggests that as film thickness increases, the breakpoint frequency decreases. Our data agree with this theory in that below the breakpoint frequency, the electrical current passed through the entire surface area including the pores, thus increasing impedance. However, our high-frequency data disagree with that of the ideal model. Our data takes into account realistic pore morphology, whereas the ideal model only accounts for uniform through-thickness pores. As a result, the

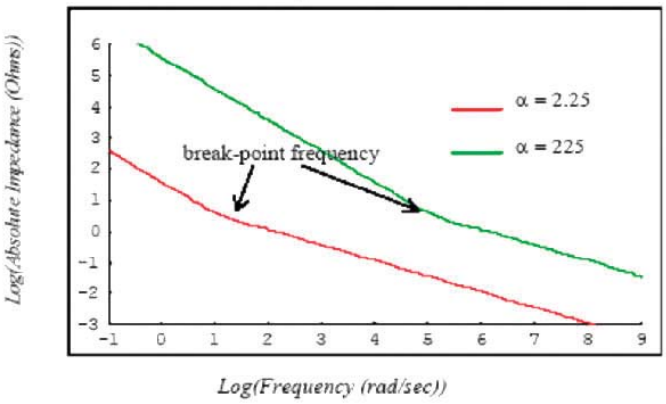

Figure 5. Model for ideal pore morphology

ideal model shows a significant decrease in the impedance at frequencies above the breakpoint frequency. Our data shows only a negligible decrease, meaning the gold acts more like a polished metal.

4. Conclusions

The results from our experiment show that as film thickness of a nanoporous metal increases, the resulting breakpoint frequency decreases. Our data agree with the ideal model in that as film thickness increases, the breakpoint frequency decreases. Yet, our data depart from the ideal model in the foreground because our data account for realistic pore morphology. As a result, the impedances at frequencies above the breakpoint frequency do not decrease as sharply as those in the ideal model.

5. Future Work

The continuation of this project is contingent upon increasing sample population of the 100 nm samples to drastically decrease the standard deviation of the breakpoint frequency. We also suggest that additional film thicknesses and the effect of varying pore size distribution on the electrochemical impedance be investigated. Lastly, we suggest that the impedance be tested with an electrolyte similar to body fluids, e.g. a Riggers solution.

Acknowledgements

We wish to thank Dr. Sean G. Corcoran of the Department of Materials Science and Engineering at Virginia Tech, for his assistance and advice throughout this project, and Mr. B. Davis Eichelberger III for his valued support in the electrochemistry and corrosion laboratory. We also want to thank Mr. Stephen McCartney for his assistance in obtaining SEM micrographs. We gratefully acknowledge Dr. G. Q. Lu of the Department of Materials Science and Engineering at Virginia Tech, for providing the silicon wafers for our samples, and Mr. Gregory Fritz for his help in the laboratory. Finally, we would like to thank Dr. Marie C. Paretti, Director of the MSE/ESM Engineering Communications Program at Virginia Tech, for helping us stay on task, on time, and organized throughout this project.

References

1. Pugh, D. V., Ph.D. thesis, Virginia Polytechnic Institute and State University, Blacksburg, VA 2003.

2. Ratner, B. D.; Hoffman, A. S.; Schoen, F. J.; Lemons, J. E., eds. *Biomaterials Science: An Introduction to Materials in Medicine*. Academic Press: 1996.

3. Dursun, A., Ph.D. thesis, Virginia Polytechnic Institute and State University, Blacksburg, VA 2003.

4. Ding, Y.; Kim, Y-J.; Erlebacher, J., Nanoporous Gold Leaf – "Ancient Technology"/Advanced Material. *Advanced Materials* **2004**, 16 (21), 1897-1900.

5. Erlebacher, J.; Aziz, M. J.; Karma, A.; Dimitrov, N.; Sieradzki, K., Evolution of Nanoporosity in Dealloying. *Nature* **2001**, 410, 450-453.

6. Erlebacher, J., An Atomistic Description of Dealloying: Porosity Evolution, the Critical Potential, and Rate-Limiting Behavior. *Journal of the Electrochemical Society* **2004**, 151, C614-C626.

7. Stratmann, M.; Rohwerder, M., A Pore View of Corrosion. *Nature* **2001**, 410, 420-423.